Research Square

Preprints are preliminary reports that have not undergone peer review.
They should not be considered conclusive, used to inform clinical practice,
or referenced by the media as validated information.

Fractal Scaling in Music and EEG Dynamics: A Detrended Fluctuation Analysis Study

Zahra Abdypour
Alzahra University
Sakineh Hosseinabadi
Sakineh.Hosseinabadi@iau.ac.ir
Islamic Azad University, East Tehran Branch
Amir Ali Masoudi
Alzahra University

Article

Keywords: Fractal Scaling, Music Features, Electroencephalography, Brain Waves, Detrended Fluctuation Analysis

Posted Date: August 3rd, 2026

DOI: https://doi.org/10.21203/rs.3.rs-10340322/v1

License: This work is licensed under a Creative Commons Attribution 4.0 International License.
Read Full License

Additional Declarations: No competing interests reported.

Fractal Scaling in Music and EEG Dynamics: A Detrended Fluctuation Analysis Study

Z. Abdypour[a], S. Hosseinabadi[b1] and A. A. Masoudi[a2]

[a] *Department of Condensed Matter Physics, Faculty of Physics, Alzahra University, Tehran, Iran*
[b] *Department of Physics, ET.C., Islamic Azad University, Tehran, Iran*

Abstract

Music exhibits complex temporal structures that often display fractal and scale-invariant properties, which may interact with the intrinsic dynamics of the human brain. In this study, we investigate the relationship between the fractal characteristics of musical features and the corresponding neural responses measured by Electroencephalography (EEG). Two musical excerpts with distinct emotional and dynamical profiles—one sentimental and calm and one epic and religious —were analyzed in terms of *Pitch, Loudness, and Rhythm* using *Detrended Fluctuation Analysis (DFA)* to quantify long-range correlations via the *Hurst exponent*. The calming music exhibits higher Hurst exponents in Rhythm and Loudness, indicating stronger long-range temporal correlations, whereas the stimulating music shows a higher Hurst exponent in Pitch, reflecting faster temporal variability. EEG signals recorded from 26 participants reveal increased scaling exponents in delta and theta bands during calming music, while stimulating music enhances beta and gamma activity and reduces temporal persistence in slower bands. These findings demonstrate a strong correspondence between the fractal organization of musical signals and the scale-dependent dynamics of brain activity.

Keewords: Fractal Scaling, Music Features, Electroencephalography, Brain Waves, Detrended Fluctuation Analysis

1 Introduction

Previous studies have demonstrated that both musical signals and neural activity exhibit fractal and scale-invariant properties across multiple temporal scales. Such properties are commonly characterized by long-range temporal correlations (LRTCs), which reflect persistent dependencies in time series data [1, 2, 3]. Detrended fluctuation analysis (DFA) has been widely employed as a robust method for quantifying these correlations in nonstationary physiological signals [4, 5, 6].

[1]Corresponding author: Sakineh.Hosseinabadi@iau.ac.ir
[2]Corresponding author: masoudi@alzahra.ac.ir

In the context of neuroscience, electroencephalography (EEG) recordings have consistently shown scale-free dynamics and long-range temporal correlations across different frequency bands, suggesting that neural activity operates near a critical state that supports flexible information processing [7, 8, 9, 10]. These fractal properties have been associated with cognitive performance, perceptual stability, and behavioral adaptability [11, 12].

Musical signals similarly exhibit complex temporal organization. Early work demonstrated that pitch and loudness fluctuations in music follow $1/f$-like statistical behavior, reflecting hierarchical temporal structure rather than random variability [13]. More recent studies have shown that rhythmic patterns across musical genres obey scale-invariant laws and display fractal fluctuations over time [14, 15]. Such temporal organization has been proposed as a key factor underlying music perception, aesthetic experience, and emotional engagement.

Despite these parallel findings, most previous research has investigated the fractal properties of musical signals and neural activity independently. Only a limited number of studies have addressed how the temporal structure of music may interact with intrinsic brain dynamics during active listening. Theoretical frameworks based on neural resonance and entrainment suggest that external rhythmic stimuli can selectively engage neural oscillations at corresponding temporal scales [16, 17, 18].

From this perspective, music characterized by strong long-range correlations and hierarchical temporal organization may preferentially entrain slow neural oscillations, whereas music with rapid temporal fluctuations may engage faster cortical dynamics. Such scale-matching mechanisms provide a plausible dynamical explanation for music–brain interactions beyond spectral content alone [19, 20, 21].

In this study, we adopt an approach grounded in statistical mechanics to directly examine the relationship between the fractal scaling properties of musical features and the corresponding dynamics of EEG activity during music perception. By applying DFA to both musical features (pitch, loudness, and rhythm) and EEG recordings obtained during listening to calming and stimulating music, we aim to provide quantitative evidence for scale-dependent coupling between external auditory temporal structures and intrinsic brain dynamics.

2 Data and Methodology

2.1 Musical Stimuli and Feature Extraction

Two globally popular musical pieces were selected for this study. Based on listeners' perceptions and prior familiarity with these works, one piece was commonly associated with religious and epic themes[3], whereas the other was generally perceived as conveying emotional and affective qualities[4]. To minimize the influence of lyrical content, instrumental versions of both pieces were

[3]https://drive.google.com/file/d/1DpDXU1aKHNFripKr9C15JXlGfDagcwuR/view?usp=sharing
[4]https://drive.google.com/file/d/12uKZw6eoE4pZHxM2psKY3UfDHy1OTXYu/view?usp=sharing

used in the analysis. Nevertheless, participants who were familiar with the original works appeared to retain similar associations and interpretations even in the absence of lyrics. These thematic characterizations therefore reflect the perceptions reported by listeners rather than objective classifications assigned by the researchers. Differences in musical dynamics can evoke distinct differential emotional and neural responses during music listening [24, 25].

The audio signals were digitized and normalized in amplitude prior to analysis. Music exhibits complex temporal organization, with fluctuations in pitch, loudness, and rhythm often displaying scale-invariant and fractal properties [13, 14].

Three musical features were extracted from each excerpt: pitch, loudness, and rhythm. Pitch was estimated as the dominant frequency over time using spectral analysis. Loudness was derived from the temporal amplitude envelope of the audio signal. Rhythmic structure was characterized by detecting beat events and computing inter-onset intervals (IOIs), which describe the temporal spacing between successive rhythmic events [15, 16, 17].

All extracted musical feature time series were subsequently analyzed using detrended fluctuation analysis (DFA) to quantify their fractal scaling behavior and enable direct comparison with EEG dynamics during music perception.

2.2 Detrended Fluctuation Analysis (DFA)

Detrended Fluctuation Analysis (DFA) is a widely used method for quantifying long-range correlations and scaling behavior in non-stationary time series. The method is particularly effective in distinguishing intrinsic correlations from trends embedded in the data[4, 5, 6].

Let $x(i)$, where $i = 1, 2, \ldots, N$, denote a one-dimensional time series of length N. The DFA procedure consists of the following steps:
Step 1: Mean Removal and Integration
First, the mean of the time series is calculated:

$$\bar{x} = \frac{1}{N} \sum_{i=1}^{N} x(i) \tag{1}$$

The time series is then transformed into an integrated profile:

$$y(k) = \sum_{i=1}^{k} \left[x(i) - \bar{x} \right], \quad k = 1, 2, \ldots, N \tag{2}$$

Step 2: Division into Non-overlapping Segments
The integrated signal $y(k)$ is divided into $N_s = \lfloor N/s \rfloor$ non-overlapping segments of equal length s, where s denotes the time scale. To account for data points at the end of the signal, the same procedure is repeated starting from the opposite end, resulting in $2N_s$ segments.
Step 3: Local Detrending

For each segment ν, a local polynomial trend $y_\nu(k)$ is fitted to the data using least-squares regression. The order of the polynomial determines the DFA order (e.g., DFA-1 for linear detrending, DFA-2 for quadratic detrending).

The detrended signal in each segment is obtained by subtracting the local trend:

$$\tilde{y}_\nu(k) = y(k) - y_\nu(k) \tag{3}$$

Step 4: Fluctuation Function
The root-mean-square fluctuation for scale s is computed as:

$$F(s) = \sqrt{\frac{1}{2N_s} \sum_{\nu=1}^{2N_s} \frac{1}{s} \sum_{k=1}^{s} \tilde{y}_\nu^2(k)} \tag{4}$$

Step 5: Scaling Behavior
The above procedure is repeated for different time scales s. If long-range power-law correlations exist in the signal, the fluctuation function follows:

$$F(s) \sim s^H \tag{5}$$

where H is the scaling exponent, also known as the DFA Hurst exponent.
Interpretation of the Scaling Exponent
The value of H characterizes the correlation properties of the time series [1, 3]:

- $H = 0.5$ indicates uncorrelated (white noise) behavior.
- $0.5 < H < 1$ indicates persistent long-range correlations.
- $H < 0.5$ indicates anti-correlated behavior.

DFA has been shown to be robust against nonstationarities such as slow trends and baseline drifts, making it particularly suitable for the analysis of biological signals, including EEG recordings [22, 6]. In the present study, DFA was applied consistently to all extracted musical features (Pitch, Loudness, and Rhythm) as well as to EEG signals in different frequency bands, allowing for a direct comparison of scaling properties across stimulus and neural domains.

2.3 EEG Acquisition and Processing

EEG data were recorded from 26 healthy participants using the international. 10–20 electrode placement system. The 10–20 system is an internationally recognized standard for EEG electrode placement, in which electrodes are positioned based on 10 percent and 20 percent intervals of the distances between specific anatomical landmarks on the scalp. This standardized arrangement ensures consistent electrode locations across subjects and enables reliable recording and comparison of brain activity. In the 10–20 system, electrode labels are assigned according to the underlying brain regions. The letters F, T, C, P, and O

denote the frontal, temporal, central, parietal, and occipital areas, respectively. Odd numbers indicate electrodes located on the left hemisphere, even numbers indicate electrodes on the right hemisphere, and the letter "z" refers to electrodes positioned along the midline of the scalp. For example, F3 represents a frontal electrode on the left hemisphere, F4 represents a frontal electrode on the right hemisphere, and Cz denotes a central electrode located on the midline. All methods were carried out in accordance with relevant guidelines and regulations. The study was performed in accordance with the guidelines approved by the Research Ethics Committee of of Alzahra University. Written informed consent was obtained from all participants prior to the experiment.

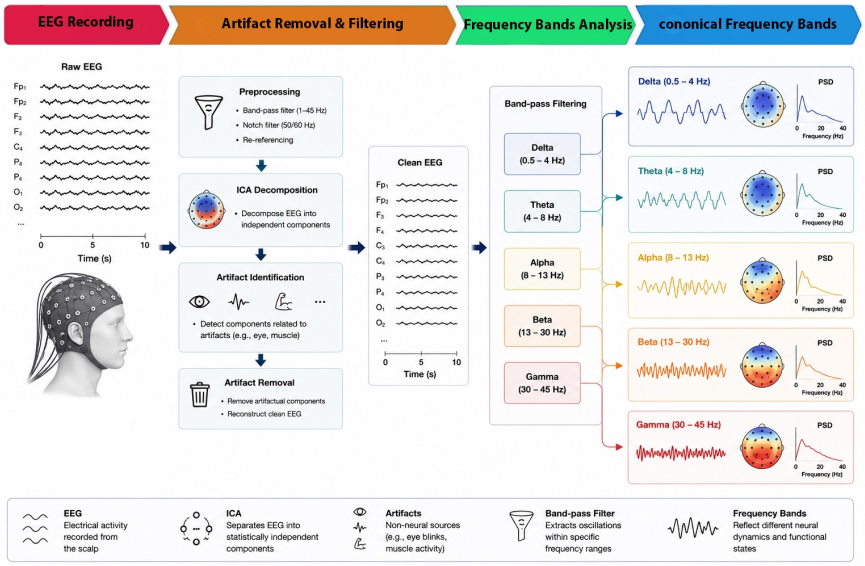


Figure 1: Schematic overview of the EEG signal processing pipeline. Raw EEG signals are first preprocessed and cleaned using independent component analysis (ICA)-based artifact removal. Subsequently, the cleaned EEG signals are decomposed into conventional frequency bands (delta, theta, alpha, beta, and gamma) for further analysis.

Signals were band-pass filtered to remove slow drifts and high-frequency noise, following standard EEG preprocessing procedures [27, 23].

Artifacts related to eye movements and muscle activity were removed using independent component analysis (ICA), after which the data were re-referenced to the common average [8, 26].

The initial EEG recordings were preprocessed using Independent Component Analysis (ICA) and a series of filtering procedures. Various sources of noise and artifacts were identified and attenuated to an acceptable extent, yielding a cleaned EEG dataset for further analysis. Initially, a 1 Hz high-pass filter was applied to remove low-frequency artifacts and baseline drifts. Subsequently, a

60 Hz low-pass filter was employed to preserve the gamma-band activity while eliminating higher-frequency noise. In addition, a 50 Hz notch filter was used to suppress power-line interference. More complex artifacts and noise components were further identified and removed using Independent Component Analysis (ICA), resulting in a cleaner EEG signal for subsequent analyses.

The cleaned EEG signals were decomposed into canonical frequency bands: delta (0.5–4 Hz), theta (4–8 Hz), alpha (8–13 Hz), beta (13–30 Hz), and gamma (30–60 Hz). Schematic overview of the EEG signal processing pipeline has been demonstrated in Fig. 1. Band-limited time series were then analyzed using detrended fluctuation analysis (DFA) to quantify long-range temporal correlations across neural rhythms [6, 7].

3 Results

3.1 Fractal Properties of Musical Features

Figure 2 shows the time series of Pitch , Loudness and Rhythm for both musical excerpts.

The corresponding DFA log–log plots for Pitch, Loudness, and Rhythm for both music conditions are shown in Fig. 3.

Figure 2 shows the time-series of Pitch, Loudness, and Rhythm for the sentimental and calm music conditions and epic and religious music conditions. The sentimental and calm music exhibits smoother temporal fluctuations, particularly in Loudness and Rhythm, whereas the epic and religious music shows faster and more irregular dynamics, most notably in Pitch.

Detrended fluctuation analysis (DFA) was applied to all musical feature time series to quantify their scaling behavior. The corresponding log–log plots are shown in Fig. 3, and Hurst exponents were estimated from the slope of the linear regions [4, 6].

For the sentimental and calm music, Loudness and Rhythm yielded higher Hurst exponents, indicating stronger long-range temporal correlations. In contrast, the epic and religious music exhibited lower Hurst exponents for these features. Pitch showed the opposite trend, with a higher Hurst exponent in the epic and religious music condition.

Overall, the two musical excerpts display distinct fractal signatures across Pitch, Loudness, and Rhythm, reflecting differences in their temporal organization.

3.2 Beat Detection, IOI Distribution, and Probabilistic Modeling of Rhythm

Figure 4 depicts the detected beat locations and the IOI distribution with its probabilistic model fitting for the rhythm signal.

The epic and religious music exhibits denser and more uniformly distributed pitch-related beat events compared to the sentimental and calm music, indicat-

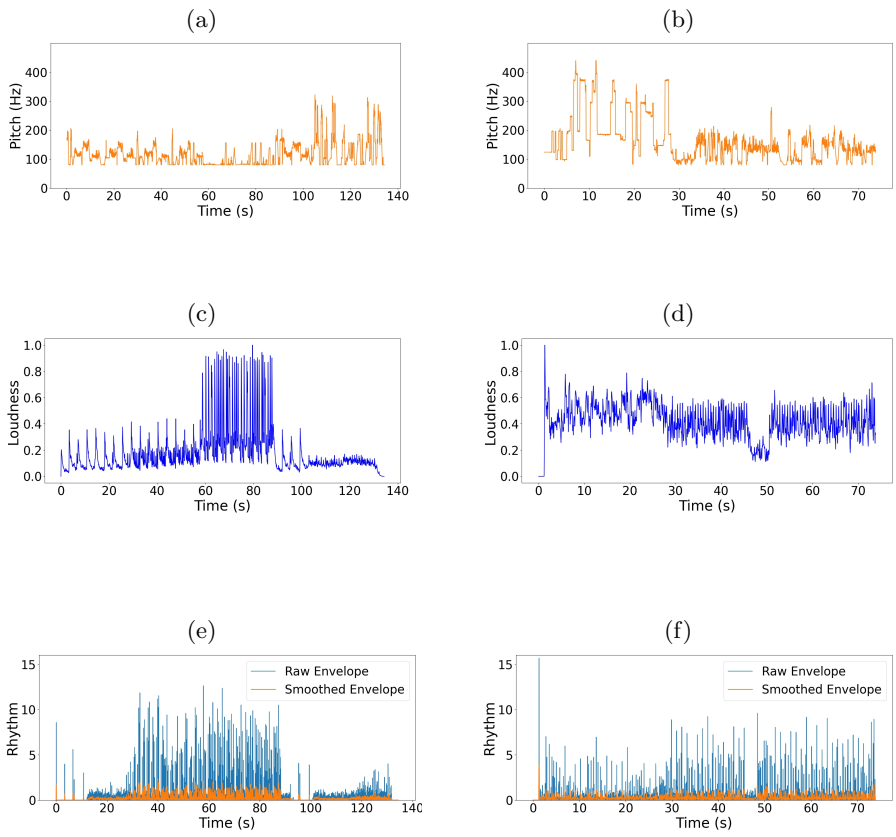


Figure 2: Time-series representations of musical features for the two musical excerpts. (a) Pitch contour of the sentimental and calm music. (b) Pitch contour of the epic and religious music. (c) Loudness contour of the sentimental and calm music. (d) Loudness contour of the epic and religious music. (e) Rhythm time series of the sentimental and calm music. (f) Rhythm time series of the epic and religious music.

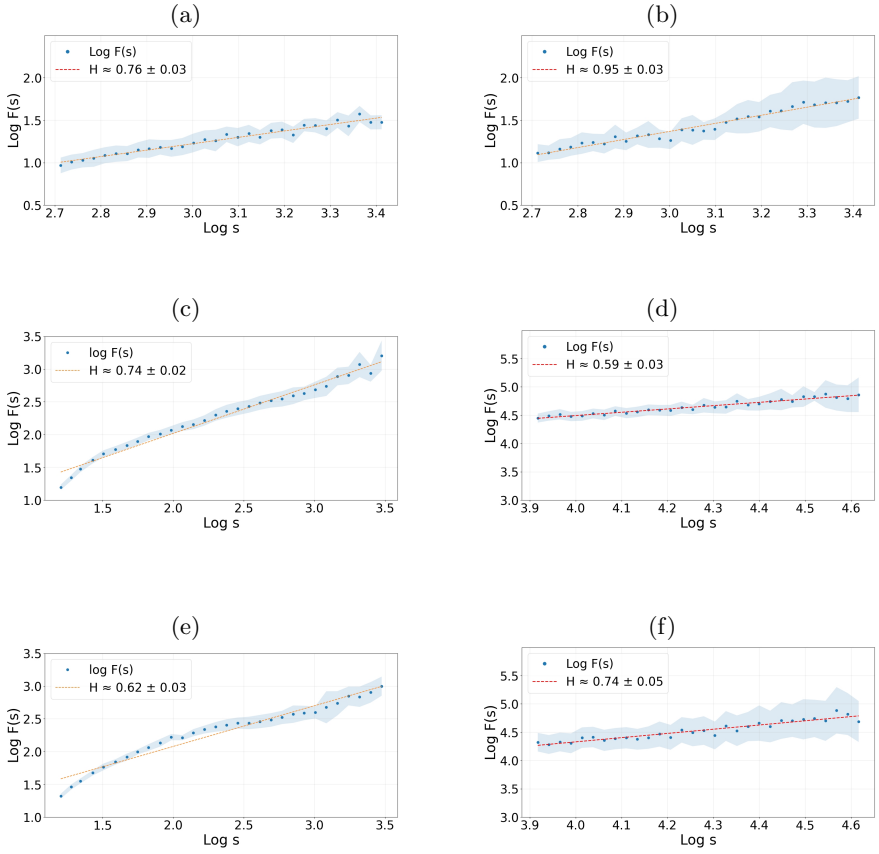


Figure 3: DFA log–log plots and estimated Hurst exponents for musical features under the two music conditions. (a) Hurst exponent estimation for Pitch in the sentimental and calm music. (b) Hurst exponent estimation for Pitch in the epic and religious music. (c) Hurst exponent estimation for Loudness in the sentimental and calm music. (d) Hurst exponent estimation for Loudness in the epic and religious music. (e) Hurst exponent estimation for Rhythm in the sentimental and calm music. (f) Hurst exponent estimation for Rhythm in the epic and religious music.

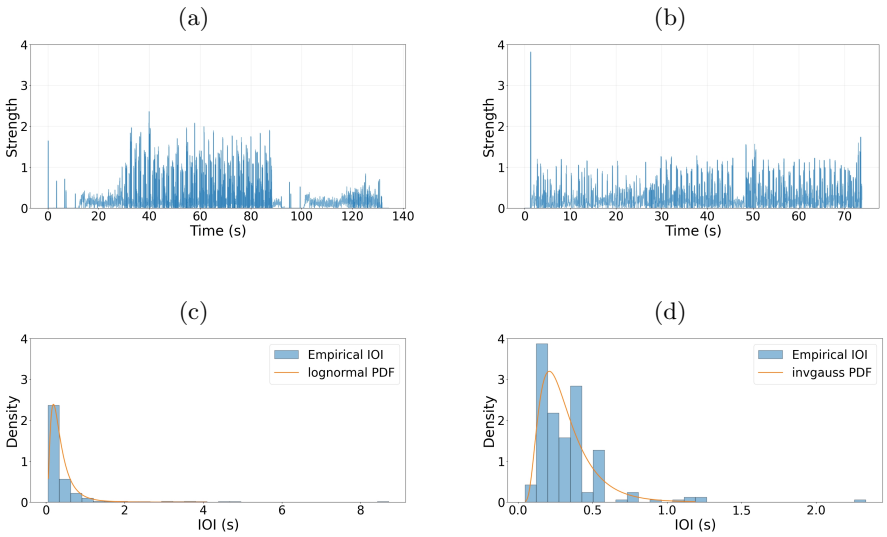


Figure 4: Beat detection and IOI distribution analysis for the two music conditions. (a) Detected beat sequence extracted from the rhythm signal of the sentimental and calm music condition. (b) Detected beat sequence extracted from the rhythm signal of the epic and religious music condition. (c) Empirical IOI distribution and probabilistic distribution fitting (log-normal) for the sentimental and calm music condition. (d) Empirical IOI distribution and probabilistic distribution fitting (inverse Gaussian) for the epic and religious music condition.

ing faster and more irregular pitch dynamics. Consistently, the IOI distribution of the sentimental and calm music follows a log-normal form, whereas the epic and religious music is better described by an inverse Gaussian distribution. Consequently, epic and religious music is associated with reduced temporal persistence and accelerated pitch transitions, while sentimental and calm music preserves a more stable, regular, and hierarchically organized temporal structure in pitch dynamics.

A comprehensive comparison of Pitch, Loudness and Rhythm is presented in Table 1.

Table 1: Comparison of acoustic and fractal characteristics between sentimental/calm vs. epic/religious music

Feature / Criterion	**Sentimental & calm**	**Epic & religious**
Loudness		
Sound intensity fluctuations	Mostly limited; brief rises	Strong, frequent variations
Temporal distribution	Calm start/end; mid-piece rise	Fluctuating throughout
Hurst exponent (H)	0.74 ± 0.05	0.59 ± 0.03
Pitch		
Frequency range	80–250 Hz	50–>400 Hz
Hurst exponent (H)	0.76 ± 0.03	0.95 ± 0.03
Rhythm		
Rhythm pattern	Regular, stable, uniform	Fast, dense, energetic
Beat density	Peak at 30–80 s; lower at ends	High overall; short, even spacing
Beat-interval (IOI) statistics	Semi-regular; log-normal; occasional long gaps	Short, dense; inverse-Gaussian; more dynamic
Hurst exponent (H)	0.74 ± 0.02	0.62 ± 0.03

3.3 EEG Scaling Behavior

Band-wise Hurst exponents and topographic maps during the sentimental and calm music condition are shown in Tab. 2 and Fig. 5, while those during the epic and religious music condition are presented in Tab. 3 and Fig. 6.

Table 2: Hurst exponent values across different EEG frequency bands during listening to the sentimental/calm music condition

Brain Region	**Delta**	**Theta**	**Alpha**	**Beta**	**Low Gamma**	**High Gamma**
Frontal	1.02 ± 0.03	0.90 ± 0.01	0.80 ± 0.02	0.62 ± 0.02	0.62 ± 0.01	0.58 ± 0.02
Temporal	1.01 ± 0.03	0.90 ± 0.01	0.80 ± 0.02	0.61 ± 0.02	0.62 ± 0.01	0.54 ± 0.02
Central	0.98 ± 0.03	0.94 ± 0.01	0.75 ± 0.02	0.63 ± 0.02	0.64 ± 0.01	0.55 ± 0.02
Parietal	0.99 ± 0.03	0.88 ± 0.01	0.77 ± 0.02	0.60 ± 0.02	0.61 ± 0.01	0.58 ± 0.02
Occipital	0.97 ± 0.03	0.96 ± 0.01	0.73 ± 0.02	0.60 ± 0.02	0.60 ± 0.01	0.56 ± 0.02

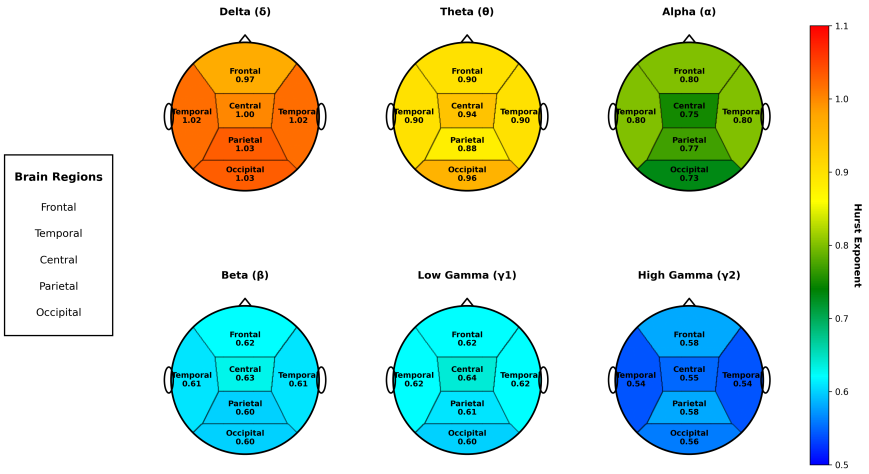


Figure 5: Topographic maps of the Hurst exponent across different brain regions and EEG frequency bands under the sentimental/calm music condition.

Table 3: Hurst exponent values across different EEG frequency bands during listening to the epic/religious music condition

Brain Region	Delta	Theta	Alpha	Beta	Low Gamma	High Gamma
Frontal	0.86 ± 0.01	0.85 ± 0.01	0.68 ± 0.02	0.67 ± 0.02	0.72 ± 0.01	0.76 ± 0.02
Temporal	0.80 ± 0.01	0.81 ± 0.01	0.68 ± 0.02	0.66 ± 0.02	0.71 ± 0.01	0.70 ± 0.02
Central	0.80 ± 0.01	0.88 ± 0.01	0.67 ± 0.02	0.65 ± 0.02	0.73 ± 0.01	0.80 ± 0.02
Parietal	0.90 ± 0.01	0.87 ± 0.01	0.71 ± 0.02	0.68 ± 0.02	0.72 ± 0.01	0.81 ± 0.02
Occipital	0.80 ± 0.01	0.88 ± 0.01	0.76 ± 0.02	0.73 ± 0.02	0.72 ± 0.01	0.90 ± 0.02

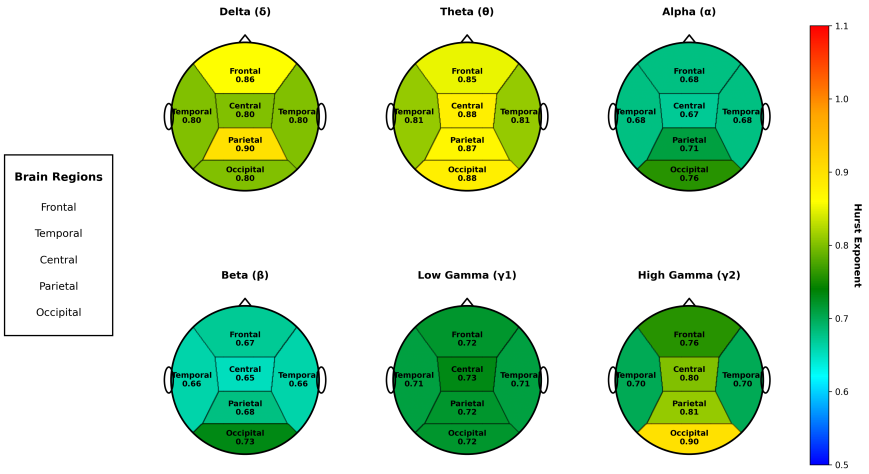


Figure 6: Topographic maps of the Hurst exponent across different brain regions and EEG frequency bands under the epic/religious music condition.

Summary table of EEG responses is presented in Table 4.

Table 4: Comparison of EEG band changes during sentimental/calm and epic/religious music

Band	**Sentimental/Calm Music**	**Epic/Religious Music**
δ	Higher; associated with relaxation.	Lower; indicates greater neural engagement.
θ	Higher; reflects internal attention.	Lower; reflects more task-oriented processing.
α	Moderate; linked to relaxation and reduced stress.	Lower; associated with increased sensory attention.
β	Moderate; indicates mild focus.	Higher; reflects greater cognitive activity and arousal.
γ	Lower; related to basic perceptual processing.	Higher; reflects complex processing and stimulation.
Summary	Relaxed state with mild focus.	Enhanced attention, cognition, and arousal.

Overall, the sentimental and calm music condition is characterized by higher Hurst exponents in low-frequency EEG bands (delta and theta), indicating stronger long-range temporal correlations associated with relaxed neural dynamics, while lower Hurst exponents are observed in higher-frequency bands (beta and gamma). In contrast, the epic and religious music condition exhibits reduced Hurst exponents in delta and theta bands, accompanied by increased Hurst exponents in beta and gamma bands, reflecting enhanced neural activation and faster temporal dynamics[7, 6].

Figure 7 shows subject-wise and averaged comparisons.

Panel (a) shows a consistent decrease in delta-band Hurst exponents during

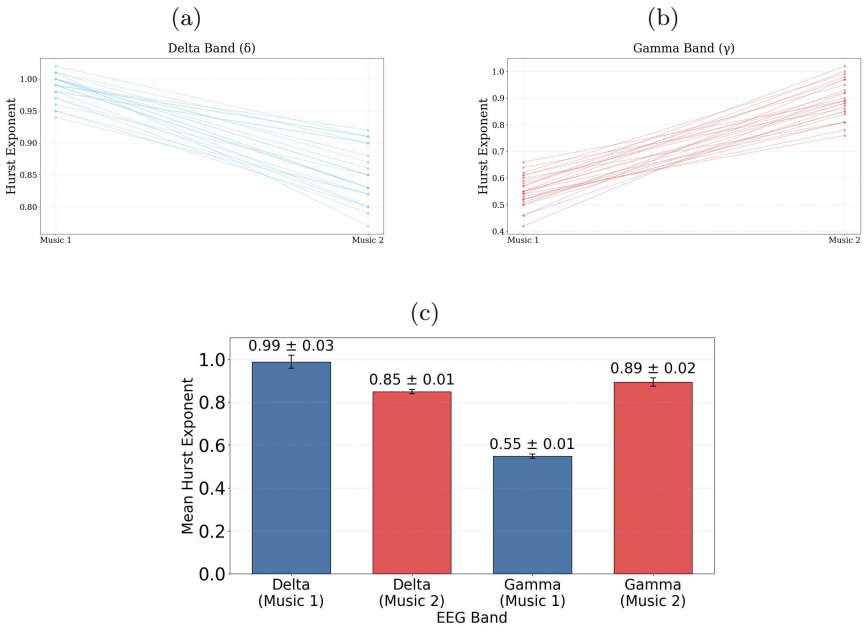


Figure 7: Subject-wise comparison of delta (a) and gamma (b) band Hurst exponents during listening to the sentimental and calm music condition(Music1) and the epic and religious music condition(Music2).(b)Mean Hurst exponents across participants for both musical conditions.

listening to the sentimental and calm music condition (Music1), accompanied by a concurrent increase in gamma-band Hurst exponents during the epic and religious music condition(Music2), indicating a shift from slow, persistent neural dynamics to faster temporal fluctuations. Panel (b) confirms this pattern at the group level, with higher delta-band scaling during the sentimental and calm music condition and enhanced gamma-band scaling during the epic and religious music condition, reflecting differential engagement of large-scale cortical processes versus fast cortical activity across the two musical conditions. The normality of paired differences was evaluated using the Shapiro–Wilk test [28]. The paired differences were normally distributed for both the delta (W = 0.936, p = 0.106) and gamma (W = 0.930, p = 0.080) bands. Therefore, paired-samples t-tests were employed [29, 30]. The delta-band Hurst exponent was significantly higher during Music 1 than Music 2 (t(25) = 12.436, p ¡ 0.001, Cohen's dz = 2.439, 95% CI [0.160, 0.223]). Conversely, the gamma-band Hurst exponent was significantly lower during Music 1 than Music 2 (t(25) = -21.363, p ¡ 0.001, Cohen's dz = -4.190, 95% CI [-0.346, -0.285]).

Table 5: Shapiro–Wilk normality test for paired differences of the Hurst exponent.

Band	**W**	**p-value**	**Normality**
Delta	0.936	0.106	Yes
Gamma	0.930	0.080	Yes

Table 6: Paired-samples t-test comparing the Hurst exponent between the two musical conditions.

Band	**t(df=25)**	**p-value**	**Cohen's d_z**	**95% CI**
Delta	12.436	< 0.001	2.439	[0.160, 0.223]
Gamma	-21.363	< 0.001	-4.190	$[-0.346, -0.285]$

These findings indicate substantial alterations in long-range temporal correlations of EEG signals between the two musical conditions.

4 Discussion

The present study provides quantitative evidence that the fractal organization of musical features is systematically reflected in the scaling behavior of EEG activity during music perception. By jointly analyzing musical signals and EEG recordings using detrended fluctuation analysis (DFA), distinct scale-dependent neural responses were observed for sentimental and calm music conditions and epic and religious music conditions.

One of the central findings of this work is the band-specific detection of long-range temporal correlations in EEG signals for two musical excerpts with

distinct emotional and dynamical profiles. Sentimental and calm music was associated with higher Hurst exponents in low-frequency bands, particularly delta and theta, indicating stronger temporal persistence and long-range correlations. Such scaling behavior has previously been linked to large-scale integrative neural processes and relaxed cognitive states [7, 6, 23].

In contrast, epic and religious music elicited reduced Hurst exponents in delta and theta bands, accompanied by increased scaling exponents in beta and gamma bands. Higher-frequency neural activity has been associated with enhanced local processing, attention, and cognitive engagement, suggesting that epic and religious music promotes faster and less temporally persistent neural dynamics [23, 8].

Importantly, these neural responses mirror the fractal properties of the musical stimuli themselves. The sentimental and calm music condition exhibited stronger long-range temporal correlations in rhythm and loudness, whereas the epic and religious music was characterized by faster pitch dynamics and reduced temporal persistence. This correspondence supports the notion of a scale-matching or temporal alignment mechanism between external auditory structures and intrinsic brain dynamics, whereby music with persistent temporal organization preferentially engages slow neural oscillations, while rapidly fluctuating musical features activate faster cortical rhythms [16, 18, 17].

Previous studies have independently reported fractal properties in musical signals and EEG activity. However, most prior work has examined these domains in isolation. The present findings extend existing literature by directly linking the fractal scaling of specific musical features to frequency-resolved EEG dynamics during active music listening [13, 14, 11].

From an applied perspective, the observed relationship between musical temporal structure and neural scaling behavior suggests that music may be systematically designed or selected to modulate specific neural states. By manipulating the fractal properties of musical features, it may be possible to influence large-scale versus fast neural dynamics in a controlled manner, with potential implications for music-based interventions and neurotechnology applications [21, 20].

5 Conclusion

This study demonstrated that the fractal scaling properties of musical features are systematically reflected in the scale-dependent dynamics of EEG activity during music perception. Using detrended fluctuation analysis (DFA), we showed that sentimental and calm music is associated with stronger long-range temporal correlations in low-frequency EEG bands, whereas epic and religious music promotes faster neural dynamics in higher frequency bands.

The observed correspondence between the temporal organization of musical features and band-specific EEG scaling supports the notion of a scale-matching mechanism between external auditory structures and intrinsic brain dynamics. These findings highlight the importance of temporal structure, beyond spectral content alone, in shaping music–brain interactions.

Overall, the present results provide a quantitative framework for understanding how different musical dynamics modulate neural activity across temporal scales and may inform future studies on music-based modulation of brain states.

6 Data Availability

The datasets used and analysed during the current study are available from the corresponding author on reasonable request.

Funding: No funding was received for conducting this study.

7 References

References

[1] Hurst, H. E. (1951). Long-term storage capacity of reservoirs. *Transactions of the American Society of Civil Engineers, 116*, 770–799.

[2] Goldberger, A. L., Amaral, L. A. N., Hausdorff, J. M., Ivanov, P. C., Peng, C. K., & Stanley, H. E. (2002). Fractal dynamics in physiology: Alterations with disease and aging. *Proceedings of the National Academy of Sciences, 99*(Suppl. 1), 2466–2472.

[3] Eke, A., Herman, P., Kocsis, L., & Kozak, L. R. (2002). Fractal characterization of complexity in temporal physiological signals. *Physiological Measurement, 23*(1), R1–R38.

[4] Peng, C. K., Havlin, S., Stanley, H. E., & Goldberger, A. L. (1995). Quantification of scaling exponents and crossover phenomena in nonstationary heartbeat time series. *Chaos, 5*(1), 82–87. https://doi.org/10.1063/1.166141

[5] Kantelhardt, J. W., Koscielny-Bunde, E., Rego, H. H. A., Havlin, S., & Bunde, A. (2001). Detecting long-range correlations with detrended fluctuation analysis. *Physica A, 295*(3–4), 441–454.

[6] Hardstone, R., Poil, S. S., Schiavone, G., Jansen, R., Nikulin, V. V., Mansvelder, H. D., & Linkenkaer-Hansen, K. (2012). Detrended fluctuation analysis: A scale-free view on neuronal oscillations. *Frontiers in Physiology, 3*, 450. https://doi.org/10.3389/fphys.2012.00450

[7] Linkenkaer-Hansen, K., Nikulin, V. V., Palva, J. M., & Ilmoniemi, R. J. (2001). Long-range temporal correlations and scaling behavior in human brain oscillations. *The Journal of Neuroscience, 21*(4), 1370–1377.

[8] Stam, C. J. (2005). Nonlinear dynamical analysis of EEG and MEG. *Clinical Neurophysiology, 116*(10), 2266–2301.

[9] He, B. J. (2011). Scale-free properties of the fMRI signal during rest and task. *The Journal of Neuroscience, 31*(39), 13786–13795.

[10] Poil, S. S., Hardstone, R., Mansvelder, H. D., & Linkenkaer-Hansen, K. (2012). Critical-state dynamics of avalanches and oscillations jointly emerge from balanced excitation/inhibition. *The Journal of Neuroscience, 32*(29), 9817–9823.

[11] Palva, J. M., Zhigalov, A., Hirvonen, J., Korhonen, O., Linkenkaer-Hansen, K., & Palva, S. (2013). Neuronal long-range temporal correlations and avalanche dynamics correlate with behavioral scaling laws. *Proceedings of the National Academy of Sciences, 110*(9), 3585–3590.

[12] Sangiuliano Intra, F., Avramiea, A.-E., Irrmischer, M., Poil, S. S., Mansvelder, H. D., & Linkenkaer-Hansen, K. (2018). Long-range temporal correlations in alpha oscillations stabilize perception. *Frontiers in Human Neuroscience, 12*, 159.

[13] Voss, R. F., & Clarke, J. (1975). 1/f noise in music and speech. *Nature, 258*, 317–318.

[14] Levitin, D. J., Chordia, P., & Menon, V. (2012). Musical rhythm spectra from Bach to Joplin obey a 1/f power law. *Proceedings of the National Academy of Sciences, 109*(10), 3716–3720.

[15] Hennig, H., Fleischmann, R., Fredebohm, A., Hagmayer, Y., Nagler, J., Witt, A., Theis, F. J., Geisel, T., & Mikhailov, A. S. (2011). The nature and perception of fluctuations in human musical rhythms. *PLOS ONE, 6*(10), e26457.

[16] Large, E. W., & Snyder, J. S. (2009). Pulse and meter as neural resonance. *Annals of the New York Academy of Sciences, 1169*, 46–57.

[17] Large, E. W., Herrera, J. A., & Velasco, M. J. (2015). Neural networks for beat perception in musical rhythm. *Frontiers in Systems Neuroscience, 9*, 159.

[18] Nozaradan, S., Peretz, I., Missal, M., & Mouraux, A. (2011). Tagging neuronal entrainment to beat and meter. *The Journal of Neuroscience, 31*(28), 10234–10240.

[19] Zatorre, R. J., Chen, J. L., & Penhune, V. B. (2007). When the brain plays music: Auditory–motor interactions. *Nature Reviews Neuroscience, 8*(7), 547–558.

[20] Hsu, C.-H., & Jung, T.-P. (2015). Neural complexity and music perception. *Frontiers in Human Neuroscience, 9*, 547.

[21] Ghosh, D., Sengupta, R., Sanyal, S., & Banerjee, A. (2019). *Musicality of human brain through fractal analytics*. Springer.

[22] Kantelhardt, J. W., Zschiegner, S. A., Koscielny-Bunde, E., Bunde, A., Havlin, S., & Stanley, H. E. (2002). Multifractal detrended fluctuation analysis of nonstationary time series. *Physica A, 316*(1–4), 87–114.

[23] Buzsáki, G. (2006). *Rhythms of the brain*. Oxford University Press.

[24] Koelsch, S. (2014). Brain correlates of music-evoked emotions. *Nature Reviews Neuroscience, 15*(3), 170–180.

[25] Juslin, P. N., & Västfjäll, D. (2008). Emotional responses to music. *Behavioral and Brain Sciences, 31*(5), 559–575.

[26] Cohen, M. X. (2014). *Analyzing neural time series data: Theory and practice*. MIT Press.

[27] Niedermeyer, E., & da Silva, F. L. (Eds.). (2005). *Electroencephalography: Basic principles, clinical applications, and related fields* (5th ed.). Lippincott Williams & Wilkins.

[28] Shapiro, S. S., Wilk, M. B. (1965). An analysis of variance test for normality (complete samples). *Biometrika 52* (3), 591–611.

[29] Cohen, J. (1988). *Statistical Power Analysis for the Behavioral Sciences*. L. Erlbaum Associates.

[30] Lakens, D. (2013). Calculating and reporting effect sizes. *Frontiers in Psychology, 4* , 863.